

A Brief Introduction to Seismic Instrumentation: Where Does My Data Come From?

Adam T. Ringler^{*1} and Patrick Bastien¹

Abstract

Modern seismology has been able to take advantage of several technological advances. These include feedback loops in the seismometer, specialized digitizers with absolute timing, and compression formats for storing data. While all of these advances have helped improve the field, they can also leave newcomers a bit confused. Our goal here is to give a brief overview of how recordings of seismic ground motion originate. We discuss the chain of events that are required to obtain digital data plus how these steps can be reversed to recover units of ground motion such as acceleration, velocity, or displacement. Finally, we show a few examples of data that have become compromised because of various non-ground-motion signals. We hope this brief overview provides a quick practical introduction to allow the reader to become familiar with the various jargon used in observational seismology.

Introduction

Observational seismology is a data-driven scientific field and has been amazingly successful at providing open-access high-quality data (Trabant *et al.*, 2012). This success comes from a combination of facts. First, high-quality instrumentation developed by manufacturers can be readily deployed. Second, the data provided by these instruments are easily accessed through data centers in a common format (Ahern *et al.*, 2009). Finally, many common software frameworks have aided in making this data-driven field more accessible and have allowed scientists to easily test new hypotheses. Although the processing methods and data sets of interest are application dependent, the instrumentation is largely standardized into a few basic types of instruments and recorders.

Although seismic instrumentation manufacturers have made instruments easy to deploy and the associated data easy to access, the instrumentation is by no means foolproof. Issues with instrumentation are further magnified by the specific study areas of interest to seismologists. While global coverage is important, seismologists are often interested in studying very remote locations that come along with harsh environments such as those found in Antarctica (Anthony *et al.*, 2015). The cost of deployments in these locations also makes it necessary for the data to be applicable to multiple different use cases. For example, the Southern Alaska Lithosphere and Mantle Observation Network (Tape *et al.*, 2017) temporary deployment was intended for imaging earth structure, but the data also found applications in studying regional noise and research regarding the constraint of local event focal mechanisms (Silwal *et al.*,

2018). These harsh locations also tend to expose instrumentation to large temperature changes as well as other environmental drivers that can compromise instrument functionality. Additionally, these environmental changes can degrade seismic data in ways that are not always obvious.

Our goal is to give a brief overview of how seismic signals are recorded from the initial ground-motion input into the seismometer along with the critical steps involved in getting the data to the end user in physically meaningful units (e.g., acceleration, velocity, or displacement). We aim to equip the reader with a basic knowledge of how seismic instruments work along with some of the associated jargon. To avoid getting bogged down in details, we only briefly touch on the instrument response, as it has been described in detail elsewhere (Aki and Richards, 2002; Stein, 2015; Havskov and Alguacil, 2016). Instead, we focus on a practical approach of using the instrument response to recover ground motion through a handful of examples. Furthermore, while we point out some of the sensitivities of seismometers to various other nonseismic noise sources, our examples are in no way comprehensive.

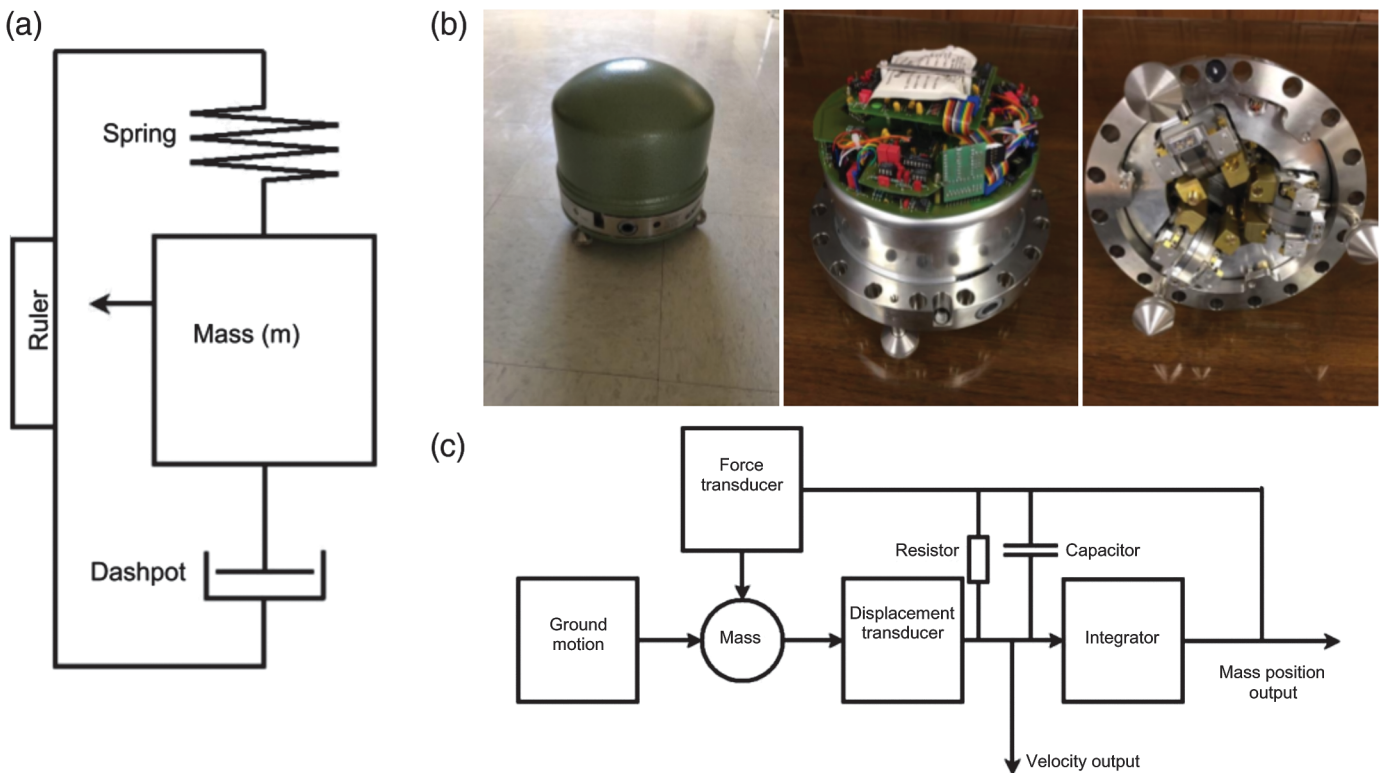
Ground to the Seismometer

Observational seismology generally begins with recording seismic waves. Once recorded, a multitude of things can then be

1. U.S. Geological Survey, Albuquerque Seismological Laboratory, Kirtland AFB, New Mexico, U.S.A.

*Corresponding author: aringler@usgs.gov

© Seismological Society of America



done with the data such as inverting for earth structure (Schmandt, 2012) or locating earthquakes (Yeck *et al.*, 2019). However, four complications arise when recording seismic waves. First, recording the motion of the ground while being located on the ground itself. Second, seismic waves span a very large bandwidth from hundreds of hertz (Hz) to lunar Earth tide periods of 80,000 s, requiring instruments to be sensitive across a large bandwidth, depending on the application. Third, seismic instruments require a huge dynamic range from a few nm/s^2 to multiple times the acceleration of Earth's gravitational field. By dynamic range, we mean range over which the instrument can operate, that is, the smallest detectable signal to the largest on-scale ground motion the instrument can record. Finally, any instrument that can record across the huge dynamic range and bandwidth just discussed also becomes sensitive to nonseismic noise sources such as temperature, pressure, and magnetic field changes.

The first issue of recording ground motion while the recording device is on the ground can be solved by a simple mechanical system where the instrument records the motion of the frame of a seismometer relative to a stationary mass (Fig. 1a) can be utilized. That is, the mass (m) is assumed stationary, and the instrument frame moves relative to the mass. We further control this by attaching the mass to the frame by way of a spring with a spring constant (k) and damping the motion by way of a dashpot with a restoring force D , which is proportional to velocity. Then, we relate the ground motion $u(t)$ as a function of the displacement of the mass relative to the frame by way of

Figure 1. (a) The mechanical principle of a seismometer where the displacement of the mass (m) is measured by a ruler on the frame of the instrument. The mass is suspended by a spring and is damped by a dashpot. (b) The Streckeisen STS-2 seismometer with the cover on, the cover off, and a view from the bottom with the cover off, respectively. (c) A feedback loop diagram of a modern-day seismometer. Ground motion displaces the seismic mass, which is recorded by a displacement transducer. This signal is then recorded as the velocity output. The differentiated signal, and RC circuit (a circuit with a resistor and capacitor), gets fed back into the mass with the opposite polarity through the force transducer. Finally, we note that the mass position output is proportional to how the mass would move if the feedback loop were to stop working. Part (c) was adapted from Wielandt (2002).

$$\ddot{x}(t)m + D\dot{x}(t) + kx(t) = -\ddot{u}(t), \quad (1)$$

in which $x(t)$ denotes the motion of the Earth in the inertial reference frame, and the dots denote differentiation with respect to time. So we record $x(t)$, but ultimately want to find $u(t)$. This differential equation can be solved in the frequency domain by making use of the Fourier transform, resulting in the following solution:

$$H(\omega) = \frac{-\omega^2}{\omega^2 + \frac{m}{D}i\omega + \frac{k}{m}}, \quad (2)$$

in which ω is the angular frequency. The function $H(\omega)$ gives the relationship between ground motion and the output of the seismometer. The responses are most easily understood

in terms of the amplitude response, which is the absolute value of $H(\omega)$ (Fig. 2a). Instead of going into further details on the solution, we point out that the fundamental limitation of this mechanical solution is the limited dynamic range. It is useful to discuss dynamic range on a logarithmic scale, because seismologists are interested in a range of signals that vary from very small signals such as the minimum Earth noise occurring with an amplitude of around 10^{-9} m/s² to the relatively large signals of a building's back-and-forth movement during a strong earthquake with accelerations multiple times that of Earth's gravitational field of 9.8 m/s². The minimum Earth noise occurs at approximately 300 s period (Zürn and Wielandt, 2007). Dealing with 10 orders of magnitude requires more convenient units, which we explain below.

Scaling units logarithmically

We take a brief intermission to discuss decibels (dBs). In fields where both very large and very small units of measure are required on the same scale, it is convenient to speak in terms of decibels. For a signal with a measurement power of P , we define P in units of dB to be given by $10 \log_{10}(P)$. When speaking about dB, it is always considered as a ratio, generally as a ratio relative to 1 unit of measure. If P is in units of acceleration squared, then $10 \log_{10}(A)$ would be in dB relative to 1 (m/s²)². The logarithmic scale allows us to compare a very large range of numbers; for example, if $P = 100,000$, we get 50 dB, and if $P = 0.000,01$, then we get -50 dB. One point of confusion is when comparing power and amplitude. We recall that the power P of a signal with amplitude A is given by $P = A^2$, which makes it possible to give the power of a signal in dB by $20 \log_{10}(A)$. Therefore, when speaking about dB, you do not need to distinguish between power and amplitude as they are the same.

If we attempt to record using the mechanical system discussed previously, as characterized by equation (1), we are limited to about 40 dB of dynamic range (Peterson and Hutt, 1989), while we can see from Figure 2b that seismologists are interested in over 144 dB of dynamic range. To better understand this huge range of measurements, it is equivalent to placing a ruler across the continental United States with markings every 0.2 m (approximately 9 inches). To circumvent the limited dynamic range of a mechanical system, most seismometer manufacturers make use of an electronic feedback loop, such as in the Streckeisen STS-2 (Fig. 2b). The idea is that instead of recording the displacement of the mass relative to the frame, the instrument records the voltage that is required to keep the mass stationary by putting a force on the mass that is proportional to the ground motion, but with a negative sign (Fig. 1c). Such electronic systems have the added benefit of allowing the manufacturer to make the sensors highly sensitive by employing operational amplifiers. An operational amplifier, also called an "op-amp," is a device used to amplify a signal within a feedback system (Horowitz and Hill, 2015). Furthermore, using an integrator, a device used to integrate the signal, allows the sensor to

have output that is proportional to velocity instead of acceleration (Wielandt, 2002). The feedback loop makes it much easier to control the response of the instrument in the electronics instead of designing more complicated mechanical systems. By shaping the response in the electronics (Fig. 2a), the manufacturer is able to deal with the dynamic ranges discussed previously as well as capture signals from a couple 100 of hertz to periods of a day at 86,400 s (Fig. 2b). While it is convenient to discuss dynamic range using a logarithmic scale, it is similarly useful to discuss frequency ranges on such a scale.

Decades and octaves

Frequency ranges are often discussed in bands by way of decades and octaves. If we are interested in a frequency band between f_1 and f_2 , then we define the number of octaves in this band to be:

$$\text{octaves} = \log_2\left(\frac{f_2}{f_1}\right).$$

Seismologists are interested in frequencies from $f_2 = 200$ Hz down to approximately $f_1 = 1.157 \times 10^{-5}$ Hz, which is over 24 octaves of bandwidth. For comparison, the human ear can generally hear in a bandwidth of about 10 octaves (Geisler, 1998). Decades are defined the same way as octaves, but you would use \log_{10} instead of \log_2 . The very large frequency band of interest also results in seismologists using period and frequency almost interchangeably depending on what is more convenient based on the frequencies (or periods) of interest.

For manufacturers to make a sensor useable over 24 octaves of bandwidth, they must shape the response so that they can get the instrument noise below Earth's background noise. Recall that every electronic instrument has some sort of intrinsic electronic noise, and all mechanical instruments have noise generated by the mechanical system (e.g., internal annealing of materials, Brownian motion, impurities in the materials producing noise). By making use of low-noise operational amplifiers and integrators, sensor manufacturers are able to shape the response of the instrument to suppress some of this noise. That is, the feedback loop in the system tries to keep the mechanical mass stationary. By doing this, the manufacturer is able to suppress some of the noise contribution coming from the mechanical portion of the sensor (Wielandt and Streckeisen, 1982). The intrinsic noise of an instrument is referred to as the self-noise of the instrument. The self-noise ultimately limits the dynamic range of the system as we are unable to record signals that have smaller amplitudes than the self-noise of the instrument. We refer the reader to Ringler *et al.* (2014) for a survey on self-noise and methods for measuring it.

We should note that it is common to speak about a sensor being flat to velocity over a certain frequency band, known as the passband. It is possible to use data with frequency content outside of the passband if the noise levels are sufficiently below the signal level of interest. However, when looking outside of

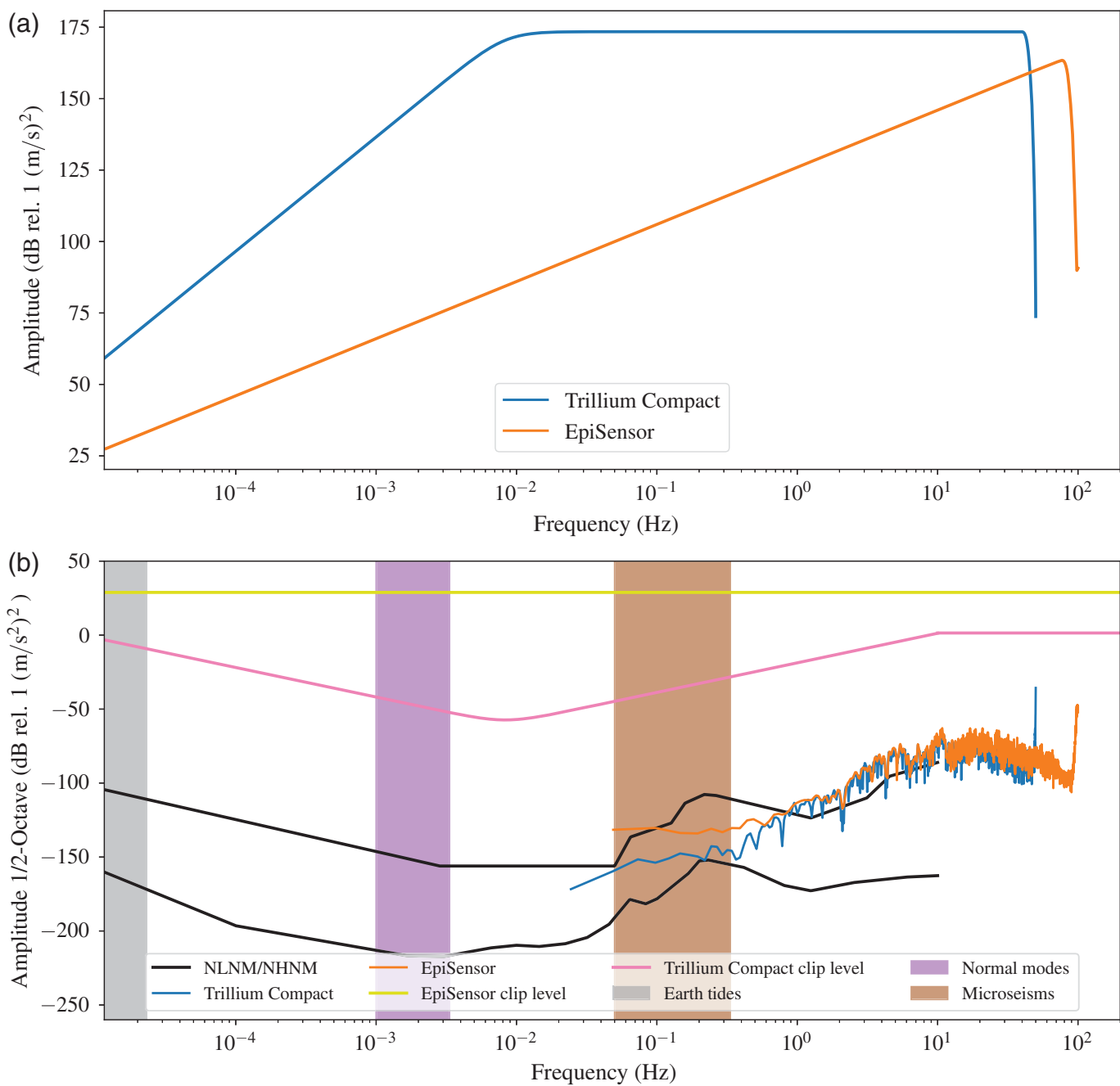


Figure 2. (a) Amplitude response in terms of velocity for a Trillium Compact (blue) and an EpiSensor (orange) as a function of frequency. The sharp decrease in both curves at very high frequencies (e.g., greater than 50 Hz) comes from the digitizer (RT-130) anti-aliasing filters. The Trillium Compact is flat to velocity to 120 s period meaning that at 120 s period (0.0083 Hz) the sensitivity is 3 dB below the sensitivity in the mid-band of the instrument. (b) A plot showing power versus frequency across a bandwidth of interest to seismologists. We highlight the lowest frequencies occurring at tidal frequencies (gray). We also show the normal-

mode frequency band (purple), along with the frequency band of the ocean-generated microseism (brown). We have included the root mean square (rms) clip levels for the Trillium Compact (pink) and the EpiSensor (yellow). We also show power spectra for a time period with a small regional event for collocated Trillium Compact (blue) and EpiSensor (orange) data. Finally, we include the Peterson (1993) new low-noise model and new high-noise model (NLNM/NHNM, black), which is representative of the smallest observed background noise and the largest observed background noise when earthquakes or other signals are not present.

the passband, the signal amplitudes are generally a function of frequency and are not flat. It is essential to always correct for the instrument response. Instrument passbands are usually

described in terms of their 3 dB points. The 3 dB point is the frequency at which the sensor's response is 3 dB below the sensitivity of the mid-band. If an instrument is flat to velocity with

a corner period of 120 s, then the instrument's response is 3 dB from the mid-band sensitivity at 120 s (Fig. 2a). This means that even when you are in the flat portion of the sensor passband you should remove the entire instrument response.

Seismometer to the Digitizer

Modern broadband seismometers will often have a voltage output range of ± 20 V. An output of 0 V corresponds to 0 m/s. An output of 20 V or -20 V means the seismometer has experienced enough motion to exceed its operational limits, which is called the clip level. The clip level is typically around 1–3 cm/s for modern broadband sensors (Fig. 2b). The clip level is determined by the maximum voltage output (± 20 V) of the sensor combined with the sensitivity of the sensor, which is the relationship between the input of the sensor to the output in the flat portion of the response. For example, a Trillium Compact has a flat response from 120 s period to approximately 100 Hz (Fig. 2a). In the region between these two frequencies, the sensor has a flat velocity output of 750 V/m/s. Compare this to the EpiSensor in Figure 2a, where the response decays with decreasing frequency. An example of clipped waveforms from 11 March 2011 M_w 9 at Global Seismographic Network (GSN) station MAJO (Matsushiro, Japan) is shown in Figure 3. The differences in the waveforms between the two collocated sensors can be attributed to the sensors having different clip levels. While this is an extreme example of clipping, the “flattened” peaks are very representative of clipped waveforms. While there are other types of seismometers, they rely on other principles (e.g., optical interferometers; Zumberge *et al.*, 2010); we restrict our attention to classic feedback seismometers.

To capture the analog output of a seismometer, we use a digitizer, which turns the analog signal into a machine-readable digital signal. The role of the digitizer is to convert this analog voltage from the broadband seismometer into a digital form of integer values commonly called counts. The amount of counts available to the digitizer is a function of the number of bits the digitizer has, which is commonly 24. The number of counts for a 24-bit digitizer is $2^{23} = 8,388,608$, with one of the bits being reserved for the sign of the signal. Typically, seismic digitizers will accept a voltage range of ± 20 V, which means 0 counts corresponds to 0 V and $-8,388,608$ counts corresponds to -20 V. From this, the bit-weight can be determined, which is the amount of voltage represented by each count; for example, $40\text{ V}/16,777,216\text{ counts} = 2.38\text{ }\mu\text{V per count}$. The sampling rate is how often the digitizer takes a voltage and converts it to counts. This is typically less than 200 Hz and is sometimes given in samples per second instead of hertz. The samples must be taken with regular intervals and aligned to Coordinated Universal Time (UTC), which is almost always done using Global Navigation Satellite Systems; however, others have attempted to implement other timing protocols (Frassetto *et al.*, 2003).

The need for digitizers to have absolute timing is one of the requirements that makes seismic digitizers expensive. However,

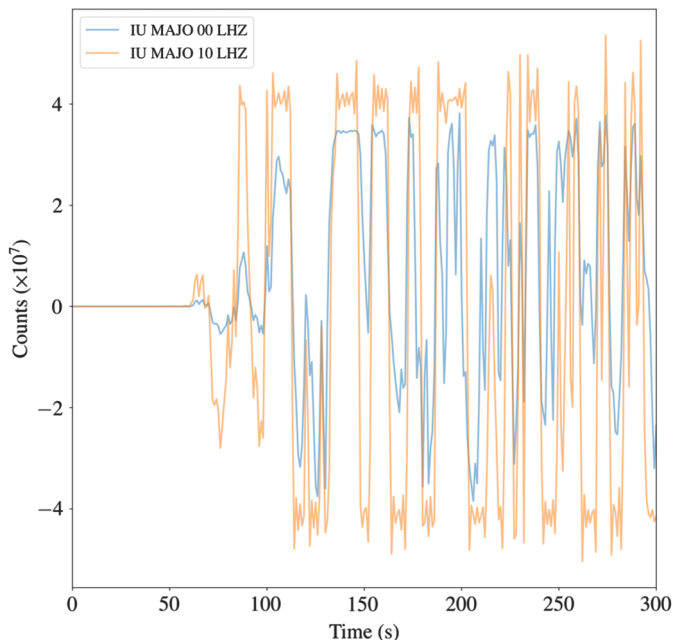


Figure 3. Waveforms from the 11 March 2011 05:46:24 M_w 9 Tohoku, Japan, earthquake at Global Seismographic Network (GSN) station MAJO (Matsushiro, Japan). The start time is the origin of the event. The station has a Streckeisen STS-1 (blue) and a Streckeisen STS-2 High-Gain (orange). The flattened peaks indicate the waveforms are being clipped because of the high accelerations.

there are a number of additional requirements that are not common in other industries. The second requirement is the need to maximize the dynamic range so that the broadband sensors with their own massive dynamic range can be fully utilized. A theoretically perfect 24-bit digitizer would have a dynamic range of 144 dB, but, in practice, due to noise the dynamic range is usually closer to 138 dB. The third special requirement is the need to minimize the power consumption because commercial power is often not available where seismic stations are installed. Some seismic digitizers now take less than 1 W to operate, which means a small car battery could power the digitizer for 2–3 days. We refer to Havskov and Alguacil (2016) for a detailed discussion of power systems. The last special requirement of seismic digitizers is the sampling frequency. The sampling rates required for seismology are in between what is commonly commercially available—either very high-rate sampling (e.g., 48,000 samples per second for audio) or very low-rate sampling (e.g., <0.1 samples per second for meteorological data). Most sample rates used in conventional seismology are below 200 samples per second and often below 100 samples per second.

Digitizer to Your Computer

With the development of digital recording equipment and with the development of the GSN in the 1980s, a standard format for seismic data was also needed; to address this need, the community developed the Standard of Earthquake Exchange

of Data (SEED). Ringler and Evans (2015) give a brief overview of the SEED format that we will not repeat here. Instead, we would like to briefly point out that the large volumes of data necessitate the use of various compression methods. For example, the Incorporated Research Institutions for Seismology Data Management Center has over 500 TB of data (see [Data and Resources](#)). The current standard uses a double differencing scheme known as Steim-2 compression, rather than storing the counts. This reduces the size of most seismic data as it makes it necessary to store smaller individual values.

For example, one day of 1 samples per second data for one channel might take 160 KB using the Steim-2 compression. However, to store these data as floats would take over 345 KB for just the data samples, not including the additional information stored in miniSEED files such as the timing, quality, and fixed section data headers.

These double-differenced data are the format that is usually shipped from data centers when a user makes a request. This was previously done through various tedious methods such as day tapes. A day tape would be all of the records from a given network for a given day. This was useful for studying a particular earthquake. However, now it is possible to get data from any available seismic station using modern webservices. For example, Figure 4 shows how to obtain data using the Python package ObsPy (Krischer et al., 2015) in nine lines of code. When this request is made, the unpackaging of the data is done and the user is left with raw counts. However, as we discussed earlier, we are really interested in units of physical ground motions such as acceleration, displacement, or velocity.

Recovering Ground Motion

Upon obtaining data in raw counts, we are left with reversing the steps previously discussed. That is, we must account for the digitizer to get units of volts. We then must correct for the response of the instrument, which will most likely have a frequency-dependent response.

An example of raw data for a local event is shown in Figure 5. These are the same data that were retrieved using the code shown in Figure 4. This station has two collocated sensors: a broadband Trillium Compact (Fig. 5, blue) and an EpiSensor accelerometer (Fig. 5, orange). While these sensors are collocated, we see that their raw count comparisons do not match (Fig. 5a). Even after correcting by the “scale factor” or the mid-band sensitivity (Fig. 5b), they appear different. One of the issues

```
#!/usr/bin/env python
from obspy.core import UTCDateTime
from obspy.clients.fdsn import Client

client = Client()
stime = UTCDateTime('2019-194T02:05:40')
etime = UTCDateTime('2019-194T02:07:00')
st = client.get_waveforms("GS", "CA03", "*",
                           "H*Z", stime, etime, attach_response = True)
```

Figure 4. Example code for retrieving data from U.S. Geological Survey (USGS, network code GS) data from station CA03, with a start time of 13 July (day of year 194) 2019 at 2:05:40 Coordinated Universal Time (UTC), for all high sample vertical components at the station. The parameters in the last two lines are the network code (GS), the station name (CA03), the location code (*), the channel codes (H*Z), the start time (stime), the end time (etime), and logical condition to include the response.

is that there is a constant offset on both sensors (e.g., the data do not have zero mean). However, in Figure 2a we see that a seismometer’s sensitivity goes to zero with decreasing frequency. This suggests that we must remove the entire frequency-dependent instrument response and not just use a single scale factor. Because the EpiSensor has units that are flat to acceleration, we need to further account for this (Fig. 5c). Finally, when the two time series from the sensors are overlain, they do not look exactly the same. This is because the EpiSensor is sampled at 200 samples per second and the Trillium Compact at 100 samples per second. Upon filtering the data (Fig. 5d), we see the data from both instruments overlay very closely. Using the same time window, we have included the half-octave integrated power in Figure 2. This allows the reader to see how these traces appear with respect to dynamic range and bandwidth. The half-octave integration allows us to compare signals on a common unit scale.

Power versus density

While we have already discussed the dB units, one important additional issue needs to be addressed. Most signals have units that are calculated in terms of an amplitude. For example, Figure 5d is in terms of mm/s^2 . However, background noise levels are usually plotted using a power spectral density (PSD), which are in units of $(\text{m}/\text{s}^2)^2/\text{Hz}$ (Fig. 6). In order to deal with this, one needs to integrate a PSD over a given bandwidth (e.g., half-octave) to get common units. This is what was done in Figure 2b. This integration can be carried out by averaging over bands, which scale by the center frequency of the band. We refer the reader to Steim (2015) for further details on frequency bandwidth integration. Comparing the new low-noise model (Peterson, 1993) and new high-noise model (Peterson, 1993) in Figure 2b with the density version in Figure 6 shows that while they have the same shape, they are different.

Although our example of recovering ground motion from raw data resulted in a very good estimate of actual ground

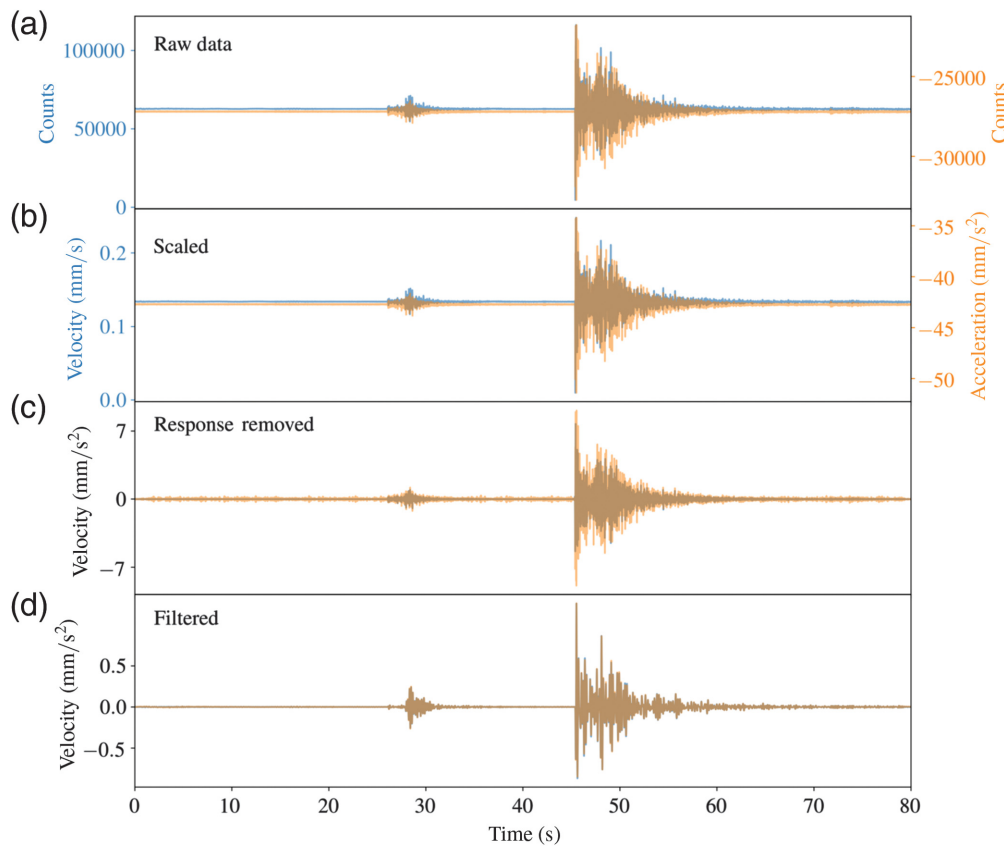


Figure 5. (a) Time series in raw counts for a small local aftershock recorded at temporary station CA03 which is part of the USGS aftershock network (network code GS) in Ridgecrest, California. The time window starts on 13 July (day of year 194) 2019 at 2:05:40 UTC. The velocity sensor is shown in blue and the accelerometer is shown in orange. (b) Same as part (a), but for both sensors scaled by their mid-band sensitivity. (c) Same as (a), but after the full instrument response has been removed. (d) Same as (c), but with a 0.1–5 Hz band-pass filtered applied to both traces. The two traces are indistinguishable in part (d) as the filter was applied to a region where the signal was above the noise of both instruments, which was not the case in part (c).

motions at the station, this need not always be the case. A multitude of things can go wrong. Recovering ground motion requires that the data and the metadata associated with the data be correct. However, it also requires that the sensor be recording ground motion with sufficient fidelity to not be compromised by local phenomena.

Recovering Non-Ground Motion

We now briefly go over a few examples of where we are unable to recover ground motion because of various “gotchas.” As we have already discussed, seismometers are highly sensitive instruments, which also makes them sensitive to temperature, pressure, magnetic fields, and other local environmental issues (Steim, 2015). Many of these factors are not obvious upon initial inspection. However, beyond outside environmental issues, it is also possible to have issues that compromise those data but are internal to the sensor.

The Streckeisen STS-2 seismometer (Fig. 2b) as well as several other instruments operate in a Galperin configuration.

That is, the instrument has three masses and each mass is tilted at a 45° angle, generally labeled U, V, and W. The output from the three sensors is then summed to provide data along two horizontal components and a vertical component. However, if something goes wrong, then the units can end up in the Galperin mode producing U, V, and W data (Fig. 6). For most well-installed broadband instruments, you can identify this issue because all three components have similar noise levels; in a good installation, the vertical component should have lower background noise levels at periods greater than 30 s. This is because the vertical is less sensitive to atmospherically induced tilt noise.

An example of tilt-induced noise is shown in Figure 6a. This is where the local barometric pressure is introducing long-period noise as the horizontal components are sensitive to tilt. This can be observed from the two horizontal-component channels LH1 (blue) and LH2 (orange) differing in

power levels from the vertical LHZ channel (green) at frequencies around 0.03 Hz. We note that because this station is located at a high latitude of 64.8° (College, Alaska), the Earth’s magnetic field changes are stronger. Because the instrument is made from ferromagnetic materials, it is sensitive to the magnetic field. However, this sensor is fairly well shielded from changes in the magnetic field. Despite this, there are cases where this is not true. For example, the KS-54000 at the GSN station QSPA (Quiet, South Pole, Antarctica) is extremely sensitive to magnetic field changes (Fig. 7). Although there are many situations where local atmospheric conditions can compromise the seismic records, there are also cases where ground motion can compromise seismic records.

When a signal with a sharp onset is recorded by a seismometer, it produces a signal that looks like the impulse response of the sensor (Fig. 8). The characteristics of the impulse response are discussed in detail in Scherbaum (2007). While such signals can come from the sensor internally clipping, it is also possible for these transients to show up with amplitudes well below

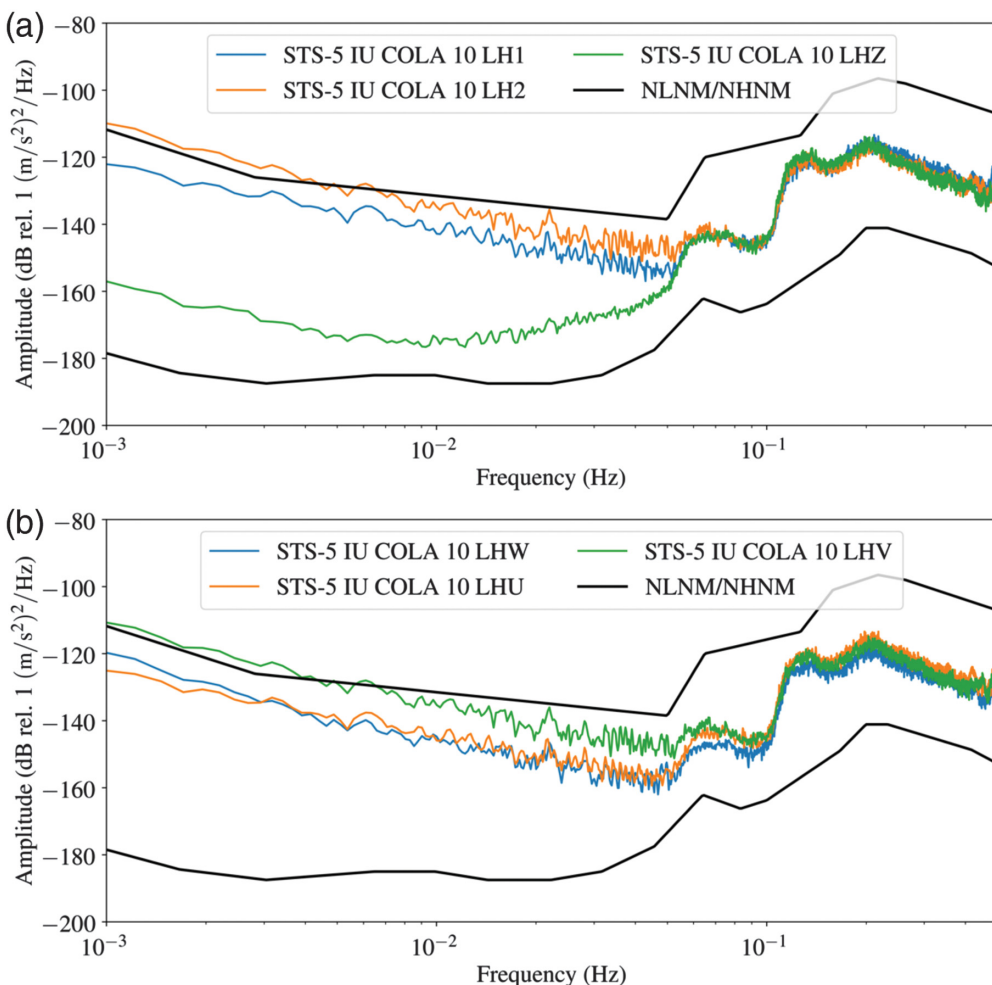


Figure 6. (a) Power spectral density plots for the STS-5 as Incorporated Research Institutions for Seismology (IRIS)/USGS (network code IU) station COLA (College, Alaska) for the three components of the sensor on 1 January 2019. (b) Same as (a), but when the sensor is in U, V, and W mode. We include the Peterson (1993) NLNM and NHNM (black) for reference.

the clip level of the sensor. Such transients can occur from the installation method (Delroy *et al.*, 2008) as well as in the internal circuitry of the sensor (Záhradník and Plešinger, 2010). The mechanisms that produce transients like those in Figure 8 are not completely understood and could be different under different scenarios. However, from the point of view of a recording ground motion, it is important to identify data with such transients as problematic and not reflective of the actual seismic wavefield at that station.

Conclusion

We have presented a brief overview of the path from the Earth shaking to how we obtain records of that shaking on a computer (Fig. 9). While these stages might be obvious to professional seismologists, we have found they are not obvious to newcomers in the field. We hope that by explaining the various steps of recovering ground motion we can aid newcomers and help them avoid common pitfalls. Finally, we highlighted a few

National Science Foundation (NSF), under Cooperative Agreement EAR-1261681. All websites were last accessed in October 2019.

Acknowledgments

This work has benefited from discussions with Rob Anthony, Geoff Bainbridge, John Evans, Andrew Holcomb, Bob Hutt, Rebecca Rodd, Joe Stein, Tyler Storm, and Dave Wilson. We thank Alexis Alejandro, Claire Doody, Alan Kafka, Debi Kilb, Jill McCarthy, Janet Slate, Carl Tape, and Jennifer Tichy for helpful reviews that improved the presentation of this work. The authors thank Debi Kilb for suggesting Figure 3, Carl Tape for suggesting Figure 8, and Claire Doody for suggesting Figure 9. The authors thank Branden Christensen for suggesting them to put together a tutorial. The authors thank their previous Albuquerque Seismological Laboratory (ASL) interns who helped them understand some of the difficulties in learning how they get ground-motion data.

Any use of trade, firm, or product names is for descriptive purposes only and does not imply endorsement by the U.S. Government.

examples of where data have become compromised because of various instrumentation issues and hope to remind data users that sometimes seismometers are recording things other than just ground motion.

Data and Resources

All data used in this work are available at the Incorporated Research Institutions for Seismology Data Management Center (IRIS DMC) (<https://ds.iris.edu/data/distribution>). We have included all codes used for making the figures on GitHub (https://github.com/aringler-usgs/Instrument_tutorial.git). We have relied heavily on the Python package ObsPy (Krischer *et al.*, 2015) as well as Matplotlib for producing colorblind-friendly figures (Hunter, 2007). The facilities of IRIS Data Services, and specifically the IRIS DMC, were used for access to waveforms, related metadata, and/or derived products used in this study. IRIS Data Services are funded through the Seismological Facilities for the Advancement of Geoscience and EarthScope (SAGE) Proposal of the National Science Foundation under Cooperative Agreement EAR-1261681. The GSN is a cooperative scientific facility operated jointly by the IRIS, the U.S. Geological Survey, and the

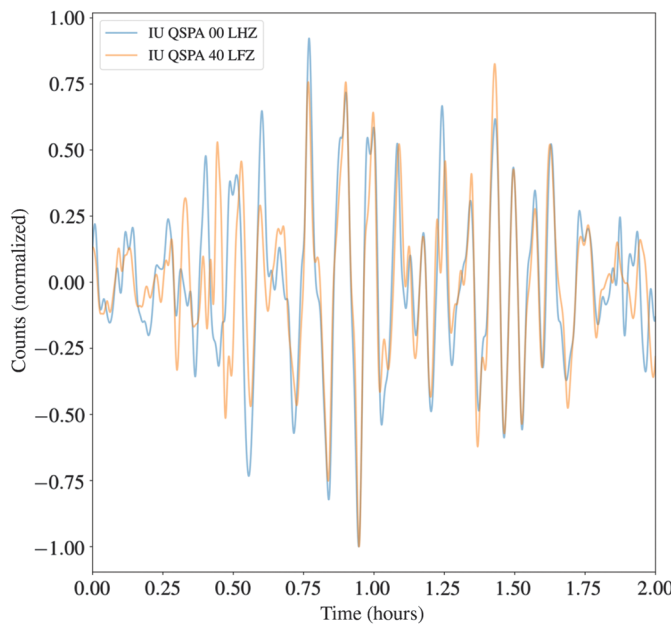


Figure 7. Vertical-component seismic data (blue) from IRIS/USGS (network code IU) station QSPA (Quiet South Pole, Antarctica) along with magnetometer data (orange) from the same location. We have normalized the counts on both units as we are only interested in the similarity of the signal, not in their amplitudes. Finally, we have band-pass filtered both traces from 0.01 to 0.002 Hz.

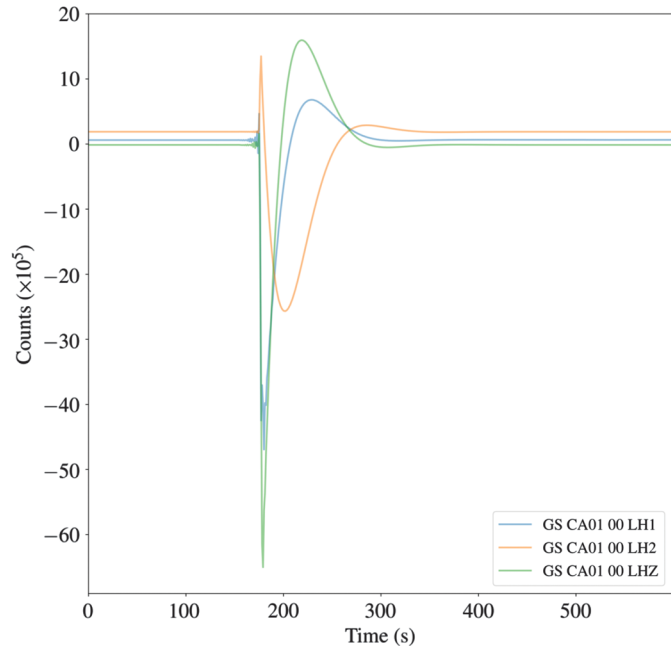


Figure 8. Example of a transient signal from temporary station CA01 which is part of the USGS aftershock network (network code GS) in Ridgecrest, California. The time window starts on 10 July 2019 at 20:07:00 UTC. We have included all three components of the broadband sensor north-south (channel LH1, blue), east-west (channel LH2, orange), and vertical (channel LHZ, green). We have removed the mean from all three traces.

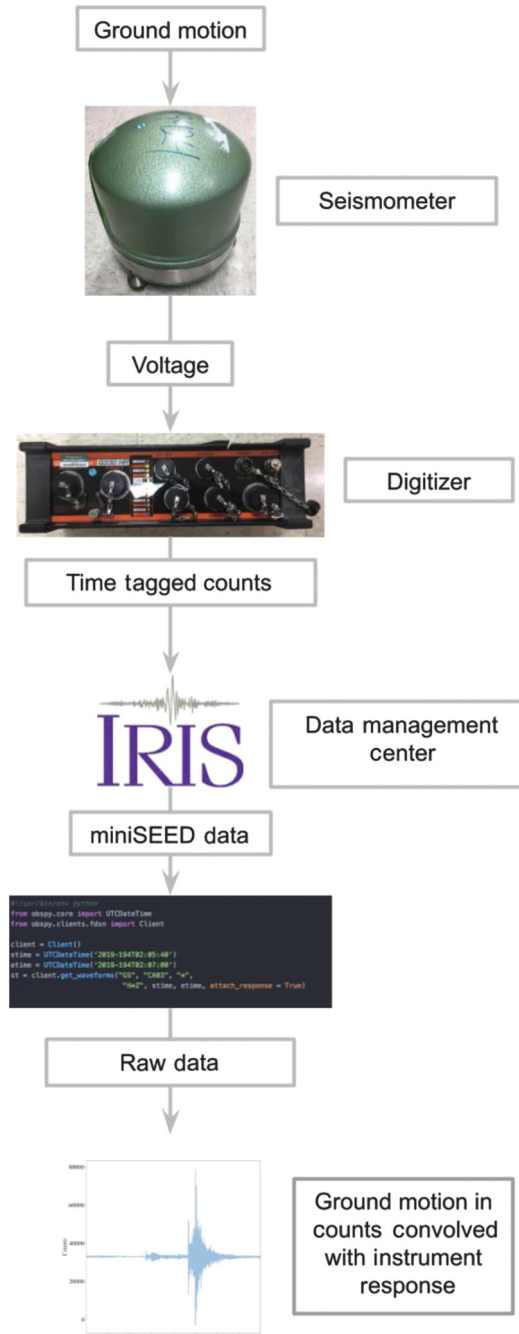


Figure 9. Summary of the steps necessary for recovering modern seismic data. Ground motion gets recorded as a voltage on a digitizer. The data are then sent to a location for archiving at the IRISDMC. Users can then request miniSEED data which, upon decoding, are in integer counts. These data contain all the contributions from the various stages of data collection including the response of the seismometer convolved with the data.

References

- Ahern, T., R. Casey, D. Barnes, R. Benson, T. Knight, and C. Trabant (2009). SEED reference manual, version 2.4, http://www.fdsn.org/seed_manual/SEEDManual_V2.4.pdf (last accessed July 2019).
- Aki, K., and P. G. Richards (2002). *Quantitative Seismology*, Second Ed., University Science Book, Sausalito, California, 700 pp.
- Anthony, R. E., R. C. Aster, D. Wiens, A. Nyblade, S. Anandakrishnan, A. Huerta, J. P. Winberry, T. Wilson, and C. Rowe (2015). The seismic noise environment of Antarctica, *Seismol. Res. Lett.* **86**, no. 1, 89–100.
- Delroy, A. A., J. Vidale, J. Stein, and P. Bodin (2008). Broadband sensor nonlinearity during moderate shaking, *Bull. Seismol. Soc. Am.* **98**, 1595–1601.
- Frassetto, A., T. J. Owens, and P. Crotwell (2003). Evaluating the Network Time Protocol (NTP) for timing in the South Carolina earth physics project (SCEPP), *Seismol. Res. Lett.* **74**, 649–652.
- Geisler, C. D. (1998). *From Sound to Synapse*, Oxford University Press, New York, New York, 396 pp.
- Havskov, J., and G. Alguacil (2016). *Instrumentation in Earthquake Seismology*, Second Ed., Springer Publishing International, Cham, Switzerland, 413 pp.
- Horowitz, P., and W. Hill (2015). *The Art of Electronics*, Third Ed., Cambridge University Press, Cambridge, United Kingdom, 1220 pp.
- Hunter, J. D. (2007). Matplotlib: A 2D graphics environment, *Comput. Sci. Eng.* **9**, no. 3, 90–95.
- Krischer, L., T. Megies, R. Barsch, M. Beyreuther, T. Lecocq, C. Caudron, and J. Wassermann (2015). Obspy: A bridge for seismology into the scientific Python ecosystem, *Comput. Sci. Discov.* **8**, doi: [10.1088/1749-4699/8/1/014003](https://doi.org/10.1088/1749-4699/8/1/014003).
- Peterson, J. (1993). Observations and modeling of seismic background noise, *U.S. Geol. Surv. Open-File Rept.* 93-322, 94 pp.
- Peterson, J., and C. R. Hutt (1989). IRIS/USGS plans for upgrading the Global Seismograph Network, *U.S. Geol. Surv. Open-File Rept.* 89-471, 46 pp.
- Ringler, A. T., and J. R. Evans (2015). A quick SEED tutorial, *Seismol. Res. Lett.* **86**, no. 6, 1717–1725.
- Ringler, A. T., R. Sleeman, C. R. Hutt, and L. S. Gee (2014). Seismometer self-noise and measuring methods, in *Encyclopedia of Earthquake Engineering*, M. Beer, A. Kougioumtzoglou, E. Patelli, and I. S-K. Au (Editors), Springer, Berlin Heidelberg, Germany, 13 pp.
- Scherbaum, F. (2007). *Of Poles and Zeros: Fundamentals of Digital Seismology*, Second Ed., Springer, Dordrecht, The Netherlands, 268 pp.
- Schmandt, B. (2012). Mantle transition zone shear velocity gradients beneath USArray, *Earth Planet. Sci. Lett.* **355–356**, 119–130.
- Silwal, V., C. Tape, and A. Lomax (2018). Crustal earthquakes in the Cook Inlet and Susitna region of southern Alaska, *Tectonophysics* **745**, 245–263.
- Steim, J. M. (2015). Theory and observations-Instrumentation for global and regional seismology, in *Treatise on Geophysics*, Second Ed., G. Schubert (Editor), Elsevier, Oxford, United Kingdom, 29–78.
- Tape, C., D. Christensen, M. M. Moore-Driskell, J. Sweet, and K. Smith (2017). Southern Alaska Lithosphere and Mantle Observation Network (SALMON): A seismic experiment covering the active arc by road, boat, plane, and helicopter, *Seismol. Res. Lett.* **88**, no. 4, 1185–1202.
- Trabant, C., A. R. Hutko, M. Bahavar, R. Karstens, T. Ahern, and R. Aster (2012). Data products at the IRIS DMC: Stepping stones for research and other applications, *Seismol. Res. Lett.* **83**, no. 5, 846–854.
- Wielandt, E. (2002). Seismic sensors and their calibration, in *New Manual of Seismological Observatory Practices*, GeoForschungs Zentrum, Potsdam, Germany, 46 pp.
- Wielandt, E., and G. Streckeisen (1982). The leaf-spring seismometer: Design and performance, *Bull. Seismol. Soc. Am.* **72**, no. 6, 2349–2367.
- Yeck, W. L., J. M. Patton, C. E. Johnson, D. Kragness, H. M. Benz, P. S. Earle, H. R. Guy, and N. B. Ambruz (2019). GLASS3: A standalone multiscale seismic detection associator, *Bull. Seismol. Soc. Am.* **109**, no. 4, 1469–1478.
- Zahradník, J., and A. Plešinger (2010). Towards understanding subtle instrumentation effects associated with weak seismic events in the near field, *Bull. Seismol. Soc. Am.* **100**, 59–73.
- Zumberge, M., J. Berger, J. Otero, and E. Wielandt (2010). An optical seismometer without force feedback, *Bull. Seismol. Soc. Am.* **100**, 598–605.
- Zürn, W., and E. Wielandt (2007). On the minimum of vertical seismic noise near 3 mHz, *Geophys. J. Int.* **168**, no. 2, 647–658.

Manuscript received 6 August 2019

Published online 29 January 2020